



HAL
open science

The junctional SR protein JP-45 affects the functional expression of the voltage-dependent Ca²⁺ channel Cav1.1.

Ayuk A. Anderson, Xavier Altafaj, Zhenlin Zheng, Zhong-Min Wang, Osvaldo Delbono, Michel Ronjat, Susan Treves, Francesco Zorzato

► To cite this version:

Ayuk A. Anderson, Xavier Altafaj, Zhenlin Zheng, Zhong-Min Wang, Osvaldo Delbono, et al.. The junctional SR protein JP-45 affects the functional expression of the voltage-dependent Ca²⁺ channel Cav1.1.. *Journal of Cell Science*, 2006, 119 (Pt 10), pp.2145-55. 10.1242/jcs.02935 . inserm-00381691

HAL Id: inserm-00381691

<https://inserm.hal.science/inserm-00381691>

Submitted on 2 Nov 2009

HAL is a multi-disciplinary open access archive for the deposit and dissemination of scientific research documents, whether they are published or not. The documents may come from teaching and research institutions in France or abroad, or from public or private research centers.

L'archive ouverte pluridisciplinaire **HAL**, est destinée au dépôt et à la diffusion de documents scientifiques de niveau recherche, publiés ou non, émanant des établissements d'enseignement et de recherche français ou étrangers, des laboratoires publics ou privés.

The junctional SR protein JP-45 affects the functional expression of the voltage-dependent Ca²⁺ channel Cav1.1

Anderson Ayuk A.¹, Altafaj Xavier², Zheng Zhenlin³, Wang Zhong-Min³, Delbono Osvaldo^{3,4}, Ronjat Michel², Treves Susan¹, Zorzato Francesco^{5*}

¹ Departments of Anaesthesia and Research Basel University Hospital, Hebelstrasse 20, 4031 Basel, CH

² Canaux calciques, fonctions et pathologies INSERM : U607, CEA : DSV/IRTSV, Université Joseph Fourier - Grenoble I, 17, rue des martyrs 38054 Grenoble, FR

³ Department of Physiology and Pharmacology, Gerontology Wake Forest University School of Medicine, Winston-Salem, NC 27157, US

⁴ Department of Internal Medicine, Gerontology Wake Forest University School of Medicine, Winston-Salem, NC 27157, US

⁵ Department of Experimental and Diagnostic Medicine University of Ferrara, General Pathology Section, Via Borsari 46, 44100 Ferrara, IT

* Correspondence should be addressed to: Francesco Zorzato <zor@unife.it>

Abstract Summary

JP-45, an integral protein of the skeletal muscle sarcoplasmic reticulum junctional face membrane, co-localizes with the sarcoplasmic reticulum calcium release channel and interacts with calsequestrin and the dihydropyridine receptor. We have identified (i) the domains of both JP-45 and of the dihydropyridine receptor involved in this interaction, and (ii) investigated the functional effect of JP-45. The cytoplasmic domain of JP-45 encompassing residues 1-80, interacts with the native dihydropyridine receptor. JP-45 interacts with two distinct and functionally relevant domains of Cav1.1 α_1 subunit, namely the I-II loop and the COOH-terminal region. The interaction between JP-45 and the I-II loop occurs via the alpha-interacting domain. The β_1a subunit also interacts with the cytosolic domain of JP-45 and its presence drastically reduces the interaction between JP-45 and the I-II loop. The functional effect of JP-45 on Cav1.1 activity was assessed by investigating charge movement in differentiated C2C12 myotubes after either overexpression or depletion of JP-45. Overexpression of JP-45 decreased peak charge movement and shifted $V_{Q1/2}$ to more negative potential (-10mV). JP-45 depletion decreased both the content of the $\alpha_1.1$ subunit and peak charge movements. Our data demonstrate that JP-45 is a protein important for functional expression of voltage dependent calcium channels.

MESH Keywords Animals ; Calcium Channels, L-Type ; biosynthesis ; metabolism ; Calsequestrin ; metabolism ; Cell Membrane ; metabolism ; Gene Silencing ; Membrane Proteins ; biosynthesis ; genetics ; metabolism ; Mice ; Muscle, Skeletal ; metabolism ; Protein Structure, Tertiary ; RNA, Messenger ; biosynthesis ; genetics ; Rabbits ; Sarcoplasmic Reticulum ; metabolism

Introduction

The skeletal muscle sarcoplasmic reticulum and the transverse tubular membranes provide a conducive environment enriched with key proteins that have been shown to play an essential role in excitation-contraction (E-C) coupling (Endo, 1985; Fleischer and Inui, 1989). E-C coupling occurs in specialized junctions called triads, which are an intracellular synapse formed by the transverse tubule membrane system and the sarcoplasmic reticulum terminal cisternae. The two main proteins involved in E-C coupling are the dihydropyridine receptor calcium channel (Cav1.1), which lies on the transverse tubules where it acts as a voltage sensor for E-C coupling, and the ryanodine receptor (RyR), present on the sarcoplasmic reticulum junctional face membrane, which is the Ca²⁺ release channel (Franzini-Armstrong and Jorgensen, 1994; Meissner, 1994; Ma and Pan, 2003; Sutko and Airey, 1996; Franzini-Armstrong, 1980; Lamb and Stephenson, 1990; Rios and Pizarro, 1991). The Cav1.1 is a hetero-oligomeric complex made up of at least four subunits: α_1 , β_1a , α_2 - δ and γ (Leung et al., 1987; Lacerda et al., 1987; Birnbaumer et al., 1998; Catterall, 1995; Snutch and Reiner, 1992). The pore-forming α_1 subunit of Cav1.1 is an integral membrane protein and is indispensable for E-C coupling, whereas the cytosolic β_1a , and α_2 - δ subunits have regulatory functions; the role of the γ subunit has yet to be clearly defined (Catterall, 1995; Snutch and Reiner, 1992; Tsien et al., 1991). The β_1a subunit associates tightly with the $\alpha_1.1$ subunit by binding to a region present on the I-II loop termed alpha interacting domain (AID) (Pragnell et al., 1994). The β_1a -subunit is important for plasma membrane expression of the $\alpha_1.1$ subunit whereas a sequence located in the COOH-domain of the $\alpha_1.1$ seems to be involved in triad targeting (Chien et al., 1995; Flucher et al., 2000; Flucher et al., 2002), though other domains/polypeptides may be involved in proper targeting.

In skeletal muscle, Cav1.1 responds to transverse tubule depolarisation by sensing the voltage change and it induces calcium release from the sarcoplasmic reticulum via a direct interaction with the RyR. Besides the RyR however, the junctional face membrane contains numerous other proteins, which, because of their anatomical location, are deemed to be involved in E-C coupling (Zhang et al., 1997; Costello et al., 1986; Zorzato et al., 2000). In the past few years a number of investigators have begun to define the major and minor structural components of the junctional face membrane (Ito et al., 2001; Takeshima et al. 2000). In previous studies (Zorzato et al., 2000; Anderson et al., 2003) we identified and characterized at the biochemical and molecular level JP-45, an integral membrane protein

constituent of the skeletal muscle sarcoplasmic reticulum junctional face membrane. We also showed that JP-45 co-localizes with the RYR calcium release channel and interacts with Cav1.1 and the luminal calcium binding protein, calsequestrin (Anderson et al., 2003). In order to gather insight into the functional role of JP-45 we defined the domains involved in the interaction between JP-45 and Cav1.1. Our results demonstrate that the cytoplasmic domain of JP-45 interacts directly with the I-II loop, the COOH-terminal domains of α 1.1 subunit as well as with the β 1a subunit. In addition we show that the interaction between JP-45 and the I-II loop occurs via the AID domain and can be displaced by β 1a. Experimental evidence has demonstrated that the β 1a subunit interacts with α 1.1 subunit via AID (Pragnell et al., 1994; Chen et al., 2004) and that this protein-protein interaction is involved in insertion of the voltage sensor to its proper membrane compartment (Flucher et al., 2002). In order to confirm the functional role of JP-45 *in vivo*, we either over-expressed or silenced endogenous JP-45 in C2C12 cells and studied the electrophysiological properties of transfected cells. Based on the results of the present report, the functional role of JP-45 is consistent with its involvement in the regulation of functional expression of the Cav1.1 into the transverse tubular membrane compartment.

Experimental procedures

Materials

PGex plasmids, nitrocellulose, rainbow Molecular Weight Markers, glutathione-Sepharose, and [³²P]dCTP were from Amersham Biosciences; goat anti- α 1 subunit of the skeletal muscle Cav1.1 polyclonal antibodies were from Santa Cruz Biotechnology Inc.; Isopropyl- β -D-thiogalactoside (IPTG), chemiluminescence kit, restriction enzymes, fugene transfection reagent, peroxidase conjugated anti-goat antibodies, EDTA-free anti-protease cocktail were from Roche Applied Science; protein-G peroxidase, protein assay determination kit and SDS-PAG protein standards were from Bio-Rad; the TALON metal affinity resins was from BD Bioscience; tricine, anti-poly-histidine, anti- β -actin Abs and peroxidase-conjugated anti-mouse antibodies were from Sigma chemicals. Jet PEI transfection reagent was from Polyplus-Transfection SAS (Illkirch, France). Protein G plus Agarose (Santa Cruz Biotechnology, Inc., Santa Cruz, CA). The pFP-N3/DsRed2 vector was constructed by in-frame substitution of the sequence encoding EGFP in the pEGFP plasmid (Clontech) with that of DsRed2. The sequence of the plasmid backbone used for subsequent cloning of JP-45 cDNA was confirmed by sequencing. All other chemicals were reagent of highest available grade.

Methods

Production and purification of fusion proteins

PCR-amplified cDNA encoding overlapping sequences of mouse skeletal muscle JP-45 were cloned in-frame into the multiple cloning site of pGex5x-3. PCR amplification conditions and primer sequences were as previously described (Anderson et al., 2003), using the following sets of primers: domain 1, encompassing residues 1-29 was amplified using the following forward and reverse primers: 5'-AGAATTCTATGACTACCAGAGGCCTGG-3' and 5'-AGTCGACGGCTGGTCCCTCCAGAAAT-3'; domain 2, encompassing residues 1-80 was amplified using the following forward and reverse primers: 5'-AGAATTCTATGACTACCAGAGGCCTGG-3' and 5'-AGTCGACTGTGCTCTCCTTGCCCGCTA-3'; domain 3, encompassing residues 81-125 was amplified using the following forward and reverse primers: 5'-AGAATTCTGGCAAAGCGGGAACAA-3' and 5'-AGTCGACATCTCCCCAGGGCAGGTC-3'; the NH₂-terminus, encompassing residues 1-125 was amplified using the following forward and reverse primers: 5'-AGAATTCTATGACTACCAGAGGCCTGG-3' and 5'-AGTCGACATCTCCCCAGGGCAGGTC-3'; the COOH-terminus, encompassing residues 149-331 was amplified using the following forward and reverse primers: 5'-AGAATTCTCGGGACGCAGTGGCT-3' and 5'-AGTCGACGTCACGCCCTTCCCTCGCTT-3'. The EcoRI restriction enzyme sequence was added to facilitate subsequent subcloning. cDNA was amplified in a Perkin Elmer GeneAmp 2400 PCR System under the following conditions: 5 min 95° C, followed by 35 cycles of 40 sec annealing at 61° C, 45 sec extension at 72° C and 30 sec denaturation at 92° C and a final elongation step of 4 min at 72° C.

The cDNAs encoding different domains of rabbit skeletal muscle α 1.1 subunit (Tanabe et al., 1987) were cloned into the pMR78 expression vector designed to express His-tagged proteins. The α 1.1 subunit constructs used include the NH₂-terminus (encompassing residues 1-51), the I-II loop (encompassing residues 335-432), the II-III loop (encompassing residues 654-797), the III-IV loop (encompassing residues 1059-1118), the proximal COOH-terminus (encompassing residues 1382-1585), the distal COOH-terminus (encompassing residues 1588-1878) and the full length β 1a subunit. All constructs were checked by direct sequencing. Plasmids were used to transform DH₂ α E. coli cells and fusion protein production was induced by the addition of 100 μ M of isopropyl- β -D-thiogalactoside (IPTG). Fusion proteins were purified according to the manufacturer's recommendations using Glutathione-Sepharose for GST-tagged fusion proteins and the TALON metal affinity resins for the His-tagged α 1.1 subunit fusion proteins. The protein concentration of the purified proteins was determined using the Bio-Rad protein assay kit and bovine serum albumin as standard (Bradford, 1976). The proteins eluted from the affinity columns were analysed by SDS-PAGE or Tricine-SDS-PAGE (Schagger and von Jagow, 1987) and visualized by either Coomassie Brilliant Blue or stained with anti-poly-histidine antibodies.

Immunoprecipitation and co-immunoprecipitation experiments

Light microsomal vesicles derived from rabbit skeletal muscle were prepared as described by Saito et al. (Saito et al., 1984). Membranes were solubilized at a final concentration of 1 mg/ml, for 30 min at room temperature in a buffer composed of 1% CHAPS, 200 mM NaCl, 1 mM dithiothreitol, 50 mM Tris-HCl pH 8.5 to which the protease inhibitor cocktail was added. Co-immunoprecipitation experiments of native proteins, was performed as previously described using the monoclonal anti-JP-45 Ab (Anderson et al. 2003). In order to identify the domain(s) of JP-45 interacting with the Cav1.1, CHAPS- solubilized light microsomal vesicles were incubated for 60 min with glutathione-Sepharose beads to which GST-JP-45 fusion proteins had been bound. Following low speed centrifugation, the beads were washed three times with PBS; bound proteins were eluted using glutathione elution buffer, separated on a 10% SDS-PAGE and transferred onto nitrocellulose. To identify JP-45 binding domains on the Cav1.1, the fusion protein encompassing domain 2 of JP-45 was immobilized on GST-Sepharose beads and incubated for 60 min with purified His-tagged fusion proteins covering various domains of the α 1.1 subunit, including the NH₂-domain, the I-II, II-III, III-IV loops, the COOH-distal and COOH-proximal domains and the β 1a domain in 10 mM HEPES and 150 mM NaCl plus anti-proteases. Beads were processed as described above.

C2C12 cells were washed with PBS, treated with 1% digitonin buffer (1% digitonin, 185 mM KCl, 1.5 mM CaCl₂, 10 mM HEPES pH 7.4) on ice for 1 hour and centrifuged at 10,000×g for 10 min at 4°C. The lysate (500µg total protein) was precleared by adding 0.5 µg of normal mouse IgG together with 20 µl of Protein G plus Agarose and incubated for 30 min on a rotating device at 4°C. After centrifugation at 2,500 rpm (1,000×g), the supernatant was transferred to a fresh tube on ice. Mouse Cav1.1 α 1 subunit primary antibody (IIF7) (kindly provided by Dr. Kevin P. Campbell, University of Iowa, Howard Hughes Medical Institute, Iowa City, IA) (Leung et al., 1987) was added and incubated at 4°C overnight. Then 20 µl Protein G plus Agarose was added to each tube and incubated for 2 hours. After centrifugation, the pellets were washed with PBS and resuspended in 20 µl of double strength sample buffer for 30 min at room temperature (Murray and Olendieck, 1997). The proteins were separated on a 10% SDS-PAGE gel and subsequently transferred onto PVDF membrane. Non-specific binding was blocked by incubating the membrane in 5% milk PBS for 60 minutes at room temperature. Incubation in the primary antibody (1:1000 diluted in blot buffer) was done for 2 hour at room temperature and washed three times for 5 min each with PBS. The membrane was incubated with anti-mouse IgG conjugated with horseradish peroxidase for 60 minutes, washed, and finally incubated in ECL Reagent and visualized in X-ray films. Autoradiograms were scanned and analyzed with KODAK-ID Image Analysis Software (Eastman Kodak Company, Rochester, NY).

Polyclonal antibody production and Western blot analysis: rabbit polyclonal antiserum was generated by immunizing a New Zealand White rabbit with glutathione-Sepharose purified GST-JP-45 fusion protein encompassing the cytoplasmic domain (aa 1-125) of JP-45. Serum was tested for the presence of Ab one month after immunization and subsequently the IgG fraction was purified by protein A column chromatography. Immunodetection of α 1.1 subunit fusion proteins was carried out using monoclonal anti-poly-Histidine antibodies, followed by peroxidase-conjugated anti-mouse IgG; immunodetection of α 1.1 subunit and JP-45 was carried out as described (Anderson et al. 2003). Immunopositive bands were visualized by chemiluminescence.

Cell Culture and transfection

The mouse C2C12 muscle cell line was obtained from American Type Culture Collection (ATCC, Rockville, MD), cultured in standard conditions and maintained in growth medium (Dulbecco's modified Eagle's medium, DMEM, supplemented with 20% foetal bovine serum, 100 units/ml penicillin and 100-µg/ml streptomycin). Cells were induced to differentiate by switching the medium to differentiation medium (DMEM supplemented with 2% horse serum, 100 units/ml penicillin and 100 µg/ml streptomycin). For overexpression experiments, C2C12 cells were transfected with the cDNA encoding JP-45, cloned in-frame into a hybrid pFP-N3/DsRed2 vector. Briefly, two days after plating, cells were transfected by adding a solution of plasmid DNA (1µg) and 3 µl FUGENE6 previously mixed for 30 min at room temperature, to the tissue culture medium. Electrophysiological measurements were made on differentiated cells 5–6 days after cell transfection. To deplete C2C12 of JP-45, we transfected cells with a JP-45 siRNA vector pSHAG. JP-45 RNA interference oligos were designed using siRNA Wizard software available at InvivoGene webpage. We choose the GCTCAACAAGTGCCTGGTACTGGCCTCGCTG nucleotides of JP-45 coding sequence. Complementary JP-45 RNAi oligos were synthesised according to instruction from Dr. G. Hannon, Cold Spring Harbor, annealed and ligated downstream U6 RNA polIII promoter of the pSHAG-1 vector as previously described (Treves et al., 2004). The nucleotide sequence of the JP-45 siRNA construct was verified by sequencing. For transfection experiments, C2C12 cells were plated on 12 mm diameter glass coverslips or on 100 mm diameter tissue culture dishes and once they reached 50–60% confluency they were transfected by a combination of CaPO₄ and Jet PEI, using a total of 7.5 µg of plasmid DNA (coverslips) or 15 µg plasmid DNA (cell culture dishes). The day after transfection, the medium was changed and the cells were allowed to recover for 24 hours. On day three the cells were induced to differentiate by switching the medium to differentiation medium (DMEM supplemented with 2% horse serum, 100 units/ml penicillin and 100 µg/ml streptomycin) and were re-transfected as described above to increase transfection efficiency. The next day fresh differentiation medium was added and cells were allowed to differentiate for another 3 days when multinucleated myotubes were clearly visible. Total RNA was extracted from transfected cells, converted into DNA as previously described (Treves et al., 2004) and RT-PCR was carried out using JP-45 specific primers or β -actin specific primers. Western blot analysis was carried out with an Ab recognising the NH₂-terminal domain of JP-45.

Charge Movement and Fluorescence Recordings

For charge movement recordings, C2C12 cells were plated on glass coverslips and mounted in a small flow-through Lucite chamber positioned on a microscope stage. Myotubes were continuously perfused with the external solution (see below) using a push-pull syringe pump (WPI, Sarasota, FL.). Cells were voltage-clamped in the whole-cell configuration of the patch-clamp (Hamill et al., 1981; Wang et al., 1999) using an Axopatch-200B amplifier (Axon Instruments/Molecular Devices, Union City, CA). Micropipettes were pulled from borosilicate glasses (Boralex) using a Flaming Brown micropipette puller (P97, Sutter Instrument Co., Novato, CA) to obtain electrode resistance ranging from 2–4 M Ω . The composition of the internal solution (pipette) was (mM): 140 Cs-aspartate; 5 Mg-aspartate₂, 10 Cs₂ EGTA (ethylene glycol-bis(α -aminoethyl ether)-N,N,N',N'-tetraacetic acid), 10 HEPES (N-[2-hydroxyethyl]piperazine-N'-[2-ethanesulfonic acid]), pH was adjusted to 7.4 with CsOH. The high concentration of Mg²⁺ in the pipette solution helped to stabilize the preparation for longer periods of time. The external solution contained (mM): 145 TEA (tetraethylammonium)-Cl, 10 CaCl₂, 10 HEPES and 0.001 tetrodotoxin. Solution pH was adjusted to 7.4 with TEA.OH. For charge movement recording, calcium current was blocked by the addition of 0.5 Cd²⁺ plus 0.3 La³⁺ to the external solution (Hamill et al., 1981; Wang et al., 1999; Wang et al., 2000; Beam and Franzini-Armstrong, 1997).

Whole-cell currents were acquired and filtered at 5 kHz with pClamp 6.04 software (Axon). A Digidata 1200 interface (Axon) was used for A–D conversion. Membrane current during a voltage pulse, P, was initially corrected by analogue subtraction of linear components. The remaining linear components were digitally subtracted on-line using hyperpolarizing control pulses of one-quarter test pulse amplitude (–P/4 procedure) (Delbono, 1992). The four control pulses were applied before the test pulse. We recorded the charge movement corresponding to gating of the L-type Ca²⁺ channel/DHPR. To this end, we used a prepulse protocol consisting of a 2-s prepulse to –30 mV and a subsequent 5-ms repolarization to a pedestal potential of –50 mV, followed by a 12.5-ms depolarization from –50 to 50 mV with 10-mV intervals (Adams et al., 1990). The optimal duration of the prepulse defined as the value at which no further immobilization of charge movement is attained, was determined to be 2 s after testing a range of prepulses from 1 to 6 s (Wang et al., 2000). Intramembrane charge movements were calculated as the integral of the current in response to depolarizing pulses (charge on, Q_{on}) and were expressed per membrane capacitance (coulombs per farad). The complete blockade of the inward calcium current was verified by the Q_{on} – Q_{off} linear relationship. Membrane capacitance was calculated as the integral of the transient current in response to a brief hyperpolarizing pulse from –80 mV (holding potential) to –100 mV.

To correlate the level of transfection with charge movement, we recorded fluorescent intensity arising from pFP-N3/DsRed2 in either JP-45 or only pFP-N3/DsRed2 transfected cells with a Radiance 2100K1 laser scanning confocal system (Zeiss, Oberkochen, Germany). Fluorescent intensity was acquired in all the areas of the cell by using a krypton laser at 568 nm and recording the emission at 640 nm. The acquisition settings, including iris aperture (used at maximum), laser intensity, exposure, and gain were maintained unmodified from cell to cell to standardize recordings and make the comparison among cells valid. The maximum fluorescent intensity of the whole cell was analyzed in digitized images and expressed in arbitrary units (AU).

Data were analyzed using Student's t test or analysis of variance (ANOVA). A value of P < 0.05 was considered significant. Data are expressed as mean \pm SEM with the number of observations (n).

Results and Discussion

Identification of interaction domains between JP-45 and Cav1.1

In a previous report we demonstrated that JP-45 interacts with the native Cav1.1 (Anderson et al., 2003). We set out a series of experiments to identify the domains participating in this interaction. We prepared recombinant GST-fusion proteins covering different coding region of JP-45 excluding the transmembrane domain (see Fig. 1), bound them to glutathione-Sepharose beads and incubated them with solubilized light microsomal vesicles. Figure 2A shows that the cytoplasmic NH₂-domain of JP-45, more specifically the region contained between residues 1-80 (domain 2) interacts with native Cav1.1. No interaction was observed between any other JP-45 domains and the Cav1.1. The physiological relevance of the interaction between fusion proteins was verified by studying the effect of GST-JP-45 domain 2 on the co-immunoprecipitation of Cav1.1 with a monoclonal anti- JP-45 Ab. The interaction between native JP-45 and Cav1.1 was competed out by the presence of soluble GST-JP-45 domain 2 in the co-immunoprecipitation reaction (fig. 2B).

Extensive structure to function relationship studies on the Cav1.1 have helped define functionally relevant domain boundaries not only among the subunits making up the supramolecular complex, but also within the primary structure of each subunit (Nakai et al., 1998; Grabner et al., 1999; Kugler et al., 2004; Van Petegem et al., 2004). We reasoned that the physiological relevance of the interaction between Cav1.1 and JP-45 could be better understood if we first identified JP-45 binding sites within the Cav1.1 α 1 subunit. JP-45 domain 2 fusion protein was immobilized on GST-Sepharose and incubated with the different His-tagged fusion proteins covering the cytoplasmic domains of the α 1.1 subunit (Tanabe et al., 1987). While some of the his-tagged fusion proteins display the expected molecular mass, in some cases they had an altered molecular mass, lower than the expected value, due to the instability of the purified fusion protein (Fig. 3A, lane 3 and 7). The protein-protein interaction experiments depicted in figure 3B demonstrate that the I–II loop and the COOH-terminal domain of the of α 1.1 subunit as well as the β 1a subunit, interact with JP-45, whereas fusion proteins corresponding to the NH₂-terminus,

the II–III and III–IV loops of the $\alpha 1.1$ subunit do not interact with GST-JP-45 domain 2 fusion protein. In order to validate these results, we performed pull-down experiments using GST-JP-45 domain 2 as bait and solubilised light microsomal vesicles as ligand, in the presence or absence of increasing concentrations of either I–II loop or COOH-distal recombinant fusion proteins. Inhibition of Cav1.1-GST-JP-45 interaction was achieved at 3.6 and 1.25 μM of I–II loop and COOH-distal his-tag fusion proteins, respectively. To further confirm the specificity of the pull-down assay, we also investigated these interactions under native conditions, i.e. by performing co-immunoprecipitation of native JP-45 with Cav1.1 using the monoclonal anti-JP-45 Ab, in the presence or absence of competing I–II loop or COOH-distal recombinant fusion proteins. As shown in figure 3D, the presence of the competing recombinant fusion proteins substantially diminished the interaction between JP-45 and the Cav1.1 domains. Pull-down and co-immunoprecipitation assays were concordant in demonstrating that competition with the single $\alpha 1.1$ interacting domains (I–II loop or COOH-distal fusion proteins) was sufficient to partially inhibit the interaction. At a first glance it may be unclear how preventing the $\alpha 1.1$ subunit-JP-45 interaction through a single domain reduces to almost zero total binding to $\alpha 1.1$ subunit. A plausible explanation of the experiments described in fig. 3C and D is that the addition of an excess of either I–II loop or COOH distal loop occupy the interacting domain of the NIC-terminal domain of JP-45. Binding of the 50 amino acid long JP-45 binding sites by an excess of either 14 kDa or 30 kDa $\alpha 1.1$ subunit loops (I–II and COOH terminal, respectively) most likely creates a steric hindrance whereby the interaction of alternative domains within the native solubilised Cav1.1 is either displaced or strongly weakened.

Immunoprecipitation experiments revealed that JP-45 interacts with the I–II loop of the $\alpha 1.1$ as well as with the purified recombinant $\beta 1a$ subunit (fig. 3B). Because the $\beta 1a$ subunit has been shown to interact strongly with the I–II loop of Cav1.1 $\alpha 1$ subunit and affect its functional expression (Flucher et al., 2000; Chien et al., 1995), in the next set of experiments we characterised in greater detail the latter protein-protein interaction.

Effect of $\beta 1a$ subunit on the interaction between JP-45 and $\alpha 1.1$ subunit

We investigated the role of the $\beta 1a$ subunit on the interaction between JP-45 and $\alpha 1.1$ subunit by both pull-down and co-immunoprecipitation assays (fig. 4). JP-45 domain 2 fusion protein was immobilized on GST-Sepharose and incubated with the His-tagged $\alpha 1.1$ subunit I–II loop fusion protein in the presence or absence of increasing concentrations of $\beta 1a$ fusion protein. As can be seen in Fig. 4A the presence of $\beta 1a$ displaces the interaction between the I–II loop and JP-45. Pull-down assays were also performed by using the solubilised light microsomal vesicles as ligand. In the latter case, the association between GST-JP-45 domain 2 and the native $\alpha 1.1$ subunit was remarkably lower in the presence of an excess of $\beta 1a$ fusion protein (Fig 4B). The displacement of the interaction between JP-45 and the $\alpha 1.1$ subunit by an excess of $\beta 1a$, was also confirmed by performing co-immunoprecipitation experiments using anti-JP-45 antibodies to pull down the native solubilised complex (Fig. 4C). These results suggest that the presence of an excess of $\beta 1a$ disrupts the complex formed between Cav1.1 and JP-45. We cannot discriminate whether JP-45 interacts either with $\alpha 1.1$ subunit or with $\beta 1a$, or whether JP-45 interacts with both subunits by forming an oligomeric complex.

The Cav1.1 $\beta 1a$ subunit has been shown to bind strongly to the intracellular loop between transmembrane domain I and II of the $\alpha 1.1$ subunit, in a region composed of 18 amino acids displaying the motif QQ-E—L-GY—WI---E which is conserved among different isoforms. (Pragnell et al., 1994). This binding domain is also referred to as AID. It is thought that the interaction between AID and the $\beta 1a$ subunit is an important determinant for the stability of the Ca^{2+} channel on the plasma membrane (Birnbaumer et al., 1998; Flucher et al., 2000; Flucher et al., 2002; Chien et al., 1995; Ahern et al., 2003; Bichet et al., 2000); in addition, the interaction between AID and $\beta 1a$ is regarded as the major structural determinant required for the surface expression of the Ca^{2+} channel (Chien et al. 1995; Beurg et al, 1999; Gregg et al., 1996; Jones et al., 1998). Co-expression of $\alpha 1.1$ and $\beta 1a$ subunits has been shown to increase the density and kinetics of L-type Ca^{2+} currents and experimental evidence suggest that the $\beta 1a$ subunit facilitates gating of the Ca^{2+} channel by increasing the coupling between charge movement and pore opening (Sheridan et al., 2003; Sheridan et al., 2004). These effects of the $\beta 1a$ subunit are due to its interaction with the I–II loop, a domain that also interacts with JP-45. In the next set of experiments we addressed the question of whether the $\beta 1a$ subunit and JP-45 share AID as binding site on the I–II loop. To address this issue we performed pull-down assays with (i) GST-I–II loop fusion protein, (ii) with a GST fusion protein encompassing AID flanked by 21 and 11 residues at the N-terminal and C-terminal ends, respectively and (iii) with a synthetic biotinylated-AID peptide. For the first two assays, GST-fusion proteins were used as bait and His-JP-45 domain 2 as ligand. The apparent molecular mass of His-JP-45 domain 2 is larger than the theoretical predicted values (approx. 31 kDa vs 14 kDa, respectively). We are confident that the apparent larger molecular mass of the His-JP-45 domain 2 fusion protein is due to the dimerisation of the fusion protein, since treatment of the His-JP-45 domain 2 with DEPC, a reagent which destroys the His tag, abolished the binding of the anti-His tag Ab (Fig. 5 panel C). Western blot analysis (Fig 5A and B) demonstrates that JP-45 domain 2 is able to interact directly with the AID sequence within the I to II loop. The *in vitro* interaction between the sequence containing AID and JP-45 occurs at micromolar concentrations JP-45 fusion protein. Because of such a high concentration, it is likely that under physiological conditions, the interaction between the $\beta 1a$ subunit and AID prevails over that of JP-45 and AID. Nevertheless, on the basis of the highly organised molecular assembly of the triad membranes, one cannot exclude the possibility that the local concentration of JP-45 in the triadic gap might be sufficient to interfere either with the high affinity interaction between the AID and $\beta 1a$ subunit (Pragnell et al., 1994; Sheridan et al., 2003; Strube et al., 1996). If there are no other proteins involved in the interaction with AID, our data imply

that in the $\beta 1a$ subunit knock-out animal AID is occupied mainly by JP-45 and that such an interaction may account, at least in part, severe phenotype of the mice (Gregg et al., 1996). Strube et al. (1996) have shown that mouse skeletal muscle cells homozygous for a null mutation in the *cchb1* gene encoding the $\beta 1a$ subunit of the Cav1.1 show a significant decrease in maximum charge movement and a shift in the half activation potential toward more negative potentials.

To investigate the functional effect of JP-45 we altered the stoichiometry of the JP-45/Cav1.1 supramolecular complex either by JP-45 overexpression or by JP-45 gene silencing in differentiated C2C12 myotubes, and then we examined Cav1.1 activity by measuring charge movement.

Effect of JP-45/DsRed2 overexpression on Cav1.1 $\alpha 1$ subunit function

To examine the expression of both JP45 and $\alpha 1.1$ subunit we carried out western blot analysis on subcellular fractions isolated from transfected cells- Fig. 6A shows a western blot of total microsome fractions from C2C12 cells transfected either with the pFP-N3/DsRed2 vector or with the JP-45/pFP-N3/DsRed2 plasmid; cells transfected with the latter plasmid show an immunoreactive band of approximately 45 kDa, which represents endogenous JP-45, and a band of approximately 70 kDa, which represents the JP-45-DsRed fusion protein. To verify whether overexpression of JP-45 affects the average content of $\alpha 1.1$ subunit we performed immunoprecipitation experiments. Total C2C12 lysate from control and JP45 overexpressing cells contain two distinct high molecular weight bands of 175 and 170 kDa referable to $\alpha 1.1$ subunit (Leung et al., 1987). The relative content of the bands did not show major change (ratio of $\alpha 1.1$ bands intensity in JP45 overexpressing cells vs those of cells expressing empty vector is 0.971 ± 0.06 , mean \pm S.D.). C2C12 cells were transfected with JP-45/pFP-N3/DsRed2 and the expression of JP-45/DsRed2 fusion protein was monitored by fluorescent microscopy to perform direct charge movement measurements. Fig. 7A shows the maximal charge movement – fluorescence relationship for C2C12 cells transfected with either JP-45/pFP-N3/DsRed2 construct (A, n = 17) or pFP-N3/DsRed2 vector alone as control (B, n = 15). As the magnitude of JP-45/DsRed2 fluorescence increased, the peak charge movement significantly decreased (A), a phenomenon that was not observed in the control cells transfected only with the pFP-3/DsRed2 plasmid (B). For the analysis of the charge movement – membrane voltage relationship of cells transfected with either JP-45/pFP-N3/DsRed2 (C) or pFP-N3/DsRed2 plasmid (D), data points were fitted to a Boltzmann equation of the form:

$$Q_{on} = Q_{max} / [1 + \exp(V_{Q1/2} - V_m) / K],$$

where Q_{max} is the maximum charge, V_m is the membrane potential, $V_{Q1/2}$ is the charge movement half – activation potential, and K is the steepness of the curve. When cells were pooled for the analysis, Q_{max} was significantly lower in JP-45/pFP-N3/DsRed2 transfected than in control cells, whereas $V_{Q1/2}$ was shifted to more negative potentials in the former group. The best fitting parameters for Q_{max} , $V_{Q1/2}$ and K recorded in both groups of cells are included in Table 1. No differences in the steepness of the curve were recorded. To better characterize the voltage-dependence of the charge movement, the group of cells transfected with JP-45/pFP-N3/DsRed2 (Fig. 7A and C) were separated into two subgroups, either exhibiting the 5 maximum or minimum Q_{max} values (Fig. 7E). This approach allows for the identification of a more obvious difference not only in Q_{max} (~3-fold) but also in the half activation potential of the charge movement (Table 1). High levels of JP-45 expression are associated with a $V_{Q1/2}$ shift to more negative potentials of ~10mV (Fig. 7C and D). No differences in the steepness of the curve were observed between these two groups of cells (Table 1).

The observation that alteration of peak charge movement is tightly linked to the magnitude of JP-45 expression suggests that the stoichiometry of the JP-45/Cav1.1 supramolecular complex is crucial for the proper function of the Cav1.1. If this is so, we reasoned that depletion of JP-45 in differentiated myotubes would similarly affect DHPR charge movement. Thus, in the next set of experiments we investigated whether charge movement is also affected in C2C12 myotubes depleted of JP-45.

Effect of JP-45 gene silencing on Cav1.1 function

The mRNA encoding JP-45 was much less abundant in C2C12 myotubes transfected with the plasmid containing JP-45 siRNA than in cells transfected with the control pSHAG vector (Fig. 8A). The presence of residual mRNA for JP-45 could be due either to the presence of a small subpopulation of cells which had not been transfected with the JP-45 siRNA construct, or to the inability of the construct to fully eliminate the transcript of JP-45. The amount of β -actin transcript did not differ significantly between cells transfected with the two constructs (fig. 8A lower panel). Western blot analysis was performed to confirm depletion of JP-45 in differentiated C2C12 myotubes. As can be seen in Fig. 8B expression of JP-45 in JP-45siRNA transfected C2C12 is lower than the detection limit of the anti- JP-45 Abs which were raised against the NH_2 -terminal interacting domain of the protein. On the other hand, we did not see changes in the expression of the house keeping gene β -actin. Having established a reduction of both transcription and expression of JP-45 we next measured Cav1.1 charge movement. C2C12 cells were co-transfected with pFP-N3/DsRed2 and either the JP-45 siRNA pSHAG vector or the pSHAG vector. Based on the expression of the reporter DsRed2 red fluorescent protein, C2C12 cells were identified and charge movement measurements were performed. Figure 9A shows that depletion of JP-45 in C2C12 myotubes is associated with a decrease in Q_{max} without apparently affecting $V_{Q1/2}$ or the steepness of the curves (Table 2). Figure 9 also shows charge movement traces recorded in C2C12 cells transfected with either pSHAG (B) or JP-45 siRNA (C), respectively. The lower Q_{max} in JP-45 depleted C2C12 cells may originate from a decrease of Cav1.1 content in muscle cell membrane. To verify this we quantified by Western blot analysis the relative content of $\alpha 1.1$ subunit in

C2C12 membrane from JP-45 siRNA and pSHAG transfected C2C12 cells. As can be seen in Fig. 9D and E, $\alpha 1.1$ subunit shows two distinct high molecular weight bands of 175 and 170 kDa (Leung et al., 1987)). Furthermore, in C2C12 myotubes depleted of JP-45, there is a significant reduction of the immunoreactive band referable to $\alpha 1.1$ subunit (Fig. 9D and Fig. 9E). The $\alpha 1.1$ subunit expression, measured as the ratio of the immunopositive band between siRNA JP-45 and control pSHAG vector transfected C2C12 cells, was 0.63 ± 0.10 (mean \pm s.e.m. $n=4$). The fractional decrease of $\alpha 1.1$ subunit expression is of 0.37 ± 0.09 and it matches the decrease in charge movement (fractional decrease: 0.34) shown in Table 2. These results indicate that JP-45 may be important for proper insertion of the $\alpha 1.1$ subunit into the muscle cell membrane.

A great deal of data have been obtained in the last few years concerning structural determinant(s) necessary for the proper functional insertion of Cav1.1 into the plasma membrane. Although all the aspects of the functional insertion into the membrane and of the targeting of the Cav1.1 are still not fully clear, the emerging idea is that cooperation of the alfa interacting domain in the I–II loop with the COOH terminal domain, in addition to the tertiary and quaternary structure assembly of the Cav1.1 complex, play a crucial role in the functional expression of the Cav1.1 α subunit in the cell membrane (Flucher et al., 2002). However, the involvement of additional protein-protein interactions between other polypeptides of the triad membrane have been implicated for the proper functional insertion of the Cav1.1 and we suggest that JP-45 is one of these additional polypeptides important for the proper assembly of the DHPR macromolecular complex into the plasma membrane.

In conclusion, in the present report we have shown that JP-45 domain 2 interacts with the AID sequence and with COOH terminal domain the Cav1.1 α subunit, two important structural determinants for functional expression of the Cav1.1. In addition, we provided clear evidence that the level of expression of JP-45 in C2C12 myotubes affects the functional properties and expression of Cav1.1. By altering the expression levels of JP-45 in differentiated C2C12 myotubes either by overexpressing its cDNA, or by JP-45 gene silencing, the stoichiometry of the JP-45/Cav1.1 supramolecular complex is dramatically altered. It is tempting to speculate that alteration of the stoichiometry of the complex influences the functional expression of the Cav1.1 by different mechanisms. Fig. 10 summarises a speculative model which describe the potential mode of action of JP-45 on Cav1.1 function and underline the importance of the correct stoichiometry of the JP-45/Cav1.1 supramolecular complex on the functional expression of Cav1.1. Overexpression of JP-45 apparently does not induce major changes in the $\alpha 1.1$ expression level, however it could enforce occupation of its binding site of the I–II loop. This occupation of the JP-45 binding site within the I–II loop may occur as consequence of a partial dissociation of the Cav1.1 $\beta 1a$ subunit, or via interaction with $\alpha 1.1$ subunit, which does not stably bind $\beta 1a$ subunit (Garcia et al., 2002; Jones et al., 2002). The I–II loop is adjacent to a repeat within the $\alpha 1.1$ subunit domain involved in channel gating. It is tempting to speculate that the effect of the overexpression and binding of JP-45 to the binding site within I–II loop is two fold:

- interference with the $\beta 1a$ action on gating currents (Strube et al., 1996, Sheridan et al., 2003);
- perturbation of the functional role of the adjacent repeat, on channel function. Each outcome, or the combination of both, would confer an inhibited conformation of the JP-45/Cav1.1 supramolecular complex leading to a decrease in charge movement. On the other hand, as indicated by Western blot analysis, depletion of JP-45 affects the total content of the Cav1.1 in the cell membrane, and in parallel also decreases maximal charge movement. The mechanism leading to the decrease in $\alpha 1.1$ subunit content in cell membranes of JP-45 depleted cells may have several explanations. Firstly, our results show JP-45 interacts with the COOH terminal domain, a region which has been shown to encompass a sequence involved in membrane targeting. When such a sequence does not interact with JP-45, proper membrane targeting of Cav1.1 may be impaired. Alternatively, JP-45 is involved in stabilising the Cav1.1 complex. The functional consequence of both events is a decrease in Q_{max} with no changes in voltage dependence of the charge movement.

JP-45 is expressed at very early stage of skeletal muscle development, in fact its transcript appears in 15 day old embryos (Anderson et al., 2003), i.e. in a developmental phase in which ER/SR membrane transition is not completed. In immature skeletal muscle fibres JP-45 might be localised in the ER/SR membrane network, and then in adult muscle fibres JP-45 is targeted to the sarcoplasmic reticulum junctional face membrane. JP-45 may be involved in the retention of the α subunit of Cav1.1 into the ER/SR membrane during the assembly of the Cav1.1 complex at an early stage of skeletal muscle development. The appearance of the $\beta 1a$ subunit will displace the interaction of between JP-45 and the I–II loop of the $\alpha 1.1$. Such an event along with the interaction of JP-45 with the COOH terminal targeting domain allow the functional expression of the $\alpha 1.1$ subunit to the transverse tubular membranes.

Acknowledgements:

This work was supported by grants from the Schweizerische Stiftung für die Erforschung der Muskelkrankheiten, from the Association Française contre les Myopathies, from the European Union, N° HPRN-CT-2002-00331 and from F.I.R.BRBAUO1ERMX, PRIN05. This work was also supported from the Department of Anaesthesia, University Hospital Basel and by grants AG18755, AG13934 and AG15820 from the National Institute of Health/National Institute on Aging, USA.

Abbreviations

AID: alpha interacting domain

Cav1.1: dihydropyridine receptor

E-C coupling: excitation-contraction coupling

RYR: ryanodine receptor

References:

- Adams BA , Tanabe T , Mikami A , Numa S , Beam KG 1990; Intramembrane charge movement restored in dysgenic skeletal muscle by injection of dihydropyridine receptor. *Nature*. 346: 569- 572
- Ahern CA , Sheridan DC , Cheng W , Mortenson L , Nataaraj P , Allen P , DeWaard M , Coronado R 2003; Ca²⁺ current and charge movements in skeletal myotubes promoted by the beta-subunit of the dihydropyridine receptor in the absence of ryanodine receptor type I. *Biophys J*. 84: 942- 959
- Anderson AA , Treves S , Biral D , Betto R , Sandona D , Ronjat M , Zorzato F 2003; The novel skeletal muscle sarcoplasmic reticulum JP-45 protein. Molecular cloning, tissue distribution, developmental expression, and interaction with alpha 1.1 subunit of the voltage-gated calcium channel. *J Biol Chem*. 278: 39987- 39992
- Beam KG , Franzini-Armstrong C 1997; Functional and structural approaches to the study of excitation-contraction coupling. *Methods Cell Biol*. 52: 283- 306
- Beurg M , Ahern CA , Vallejo P , Conklin MW , Powers PA , Gregg RG , Coronado R 1999; Involvement of the carboxy-terminus region of the dihydropyridine receptor beta1a subunit in excitation-contraction coupling of skeletal muscle. *Biophys J*. 77: 2953- 2967
- Bichet D , Cornet V , Geib S , Carlier E , Volsen S , Hoshi T , Mori Y , DeWaard M 2000; The I-II loop of the Ca²⁺ channel alpha1 subunit contains an endoplasmic reticulum retention signal antagonized by the beta subunit. *Neuron*. 25: 177- 190
- Birnbaumer L , Qin N , Olcese R , Tareilus E , Platano D , Costantin J , Stefani E 1998; Structures and functions of calcium channel beta subunits. *J Bioenerg Biomemb*. 30: 357- 375
- Bradford MM 1976; A rapid and sensitive method for the quantitation of microgram quantities of protein utilizing the principle of protein-dye binding. *Anal Biochem*. 72: 248- 254
- Catterall WA 1995; Structure and function of voltage-gated ion channels. *Annu Rev Biochem*. 64: 493- 531
- Chen Y , Li M , Zhang Y , He L , Yamada Y , Fitzmaurice A , Shen Y , Zhang H , Tong L , Yang J 2004; Structural basis of the alpha1-beta subunit interaction of voltage-gated Ca²⁺ channels. *Nature*. 429: 675- 680
- Chien AJ , Zhao X , Shirokov RE , Puri TS , Chang CF , Sun D , Rios E , Hosey MM 1995; Roles of a membrane-localized beta subunit in the formation and targeting of functional L-type Ca²⁺ channels. *J Biol Chem*. 270: 30036- 30044
- Costello B , Chadwick C , Saito A , Chu A , Maurer A , Fleischer S 1986; Characterization of the junctional face membrane from terminal cisternae of sarcoplasmic reticulum. *J Cell Biol*. 103: 741- 753
- Delbono O 1992; Calcium current activation and charge movement in denervated mammalian skeletal muscle fibres. *J Physiol (Lond)*. 451: 187- 203
- Endo M 1977; Calcium release from sarcoplasmic reticulum. *Physiol Rev*. 57: 71- 108
- Fleischer S , Inui M 1989; Biochemistry and biophysics of excitation-contraction coupling. *Annu Rev Biophys Biophys Chem*. 18: 333- 3644
- Flucher BE , Kasielk N , Grabner M 2000; The triad targeting signal of the skeletal muscle calcium channel is localized in the COOH terminus of the alpha(1S) subunit. *J Cell Biol*. 151: 467- 478
- Flucher BE , Weiss RG , Grabner M 2002; Cooperation of two-domain Ca(2+) channel fragments in triad targeting and restoration of excitation- contraction coupling in skeletal muscle. *Proc Natl Acad Sci USA*. 99: 10167- 10172
- Franzini-Armstrong C 1980; Structure of sarcoplasmic reticulum. 39: 2403- 2409
- Franzini-Armstrong CA , Jorgensen AO 1994; Structure and development of E-C coupling units in skeletal muscle. *Annu Rev Physiol*. 56: 509- 534
- Garcia R , Carrillo E , Rebolledo S , Garcia MC , Sanchez JA 2002; The beta1a subunit regulates the functional properties of adult frog and mouse L-type Ca²⁺ channels of skeletal muscle. *J Physiol*. 545: 407- 419
- Grabner M , Dirksen RT , Suda N , Beam KG 1999; The II-III loop of the skeletal muscle dihydropyridine receptor is responsible for the Bi-directional coupling with the ryanodine receptor. *J Biol Chem*. 274: 21913- 21919
- Gregg RG , Meissing A , Strube C , Beurg M , Moss R , Behan M , Sukhareva M , Haynes S , Powell JA , Coronado R , Powers PA 1996; Absence of the beta subunit (cchb1) of the skeletal muscle dihydropyridine receptor alters expression of the alpha 1 subunit and eliminates excitation-contraction coupling. *Proc Natl Acad Sci USA*. 93: 13961- 13966
- Hamill OP , Marty A , Neher E , Sakmann B , Sigworth FJ 1981; Improved patch-clamp techniques for high-resolution current recording from cells and cell-free membrane patches. *Pflugers Arch*. 391: 85- 100
- Ito K , Komazaki S , Sasamoto K , Yoshida M , Nishi M , Kitamura K , Takeshima H 2001; Deficiency of triad junction and contraction in mutant skeletal muscle lacking junctophilin type 1. *J Cell Biol*. 154: 1059- 1067
- Kugler G , Weiss RG , Flucher BE , Grabner M 2004; Structural requirements of the dihydropyridine receptor alpha 1S II-III loop for skeletal-type excitation-contraction coupling. *J Biol Chem*. 279: 4721- 4728
- Jones LP , Wei AK , Yue DT 1998; Mechanism of auxiliary subunit modulation of neuronal alpha1E calcium channels. *J Gen Physiol*. 112: 125- 143
- Jones SW 2002; Calcium channels: when is a subunit not a subunit?. *J Physiol*. 545: 33-
- Ma J , Pan Z 2003; Junctional membrane structure and store operated calcium entry in muscle cells. *Front Biosci*. 8: d242- d255
- Meissner G 1994; Ryanodine receptor/Ca²⁺ release channels and their regulation by endogenous effectors. *Annu Rev Physiol*. 56: 485- 508
- Murray BE , Ohlendieck K 1997; Cross-linking analysis of the ryanodine receptor and alpha1-dihydropyridine receptor in rabbit skeletal muscle triads. *Biochem J*. 324: 689- 696
- Nakai J , Sekiguchi N , Rando TA , Allen PD , Beam KG 1998; Two regions of the ryanodine receptor involved in coupling with L-type Ca²⁺ channels. *J Biol Chem*. 273: 13403- 13406
- Lacerda AE , Kim HS , Ruth P , Perez-Reyes E , Flockerzi V , Hofmann F , Birnbaumer L , Brown AM 1991; Normalization of current kinetics by interaction between the alpha 1 and beta subunits of the skeletal muscle dihydropyridine-sensitive Ca²⁺ channel. *Nature*. 352: 527- 530
- Lamb GD , Stephenson DG 1990; Control of calcium release and the effect of ryanodine in skinned muscle fibres of the toad. *J Physiol (Lond)*. 423: 519- 542
- Leung AT , Imagawa T , Campbell KP 1987; Structural characterization of the 1,4-dihydropyridine receptor of the voltage-dependent Ca²⁺ channel from rabbit skeletal muscle. Evidence for two distinct high molecular weight subunits. *J Biol Chem*. 262: 7943- 6
- Pragnell M , De Waard M , Mori Y , Tanabe T , Snutch TP , Campbell KP 1994; Calcium channel beta-subunit binds to a conserved motif in the I-II cytoplasmic linker of the alpha 1-subunit. *Nature*. 368: 67- 70
- Saito A , Seiler S , Chu A , Fleischer S 1984; Preparation and morphology of sarcoplasmic reticulum terminal cisternae from rabbit skeletal muscle. *J Cell Biol*. 99: 875- 885
- Schagger H , von Jagow G 1987; Tricine-sodium dodecyl sulfate-polyacrylamide gel electrophoresis for the separation of proteins in the range from 1 to 100 kDa. *Anal Biochem*. 166: 368- 379
- Sheridan DC , Cheng W , Ahern CA , Mortenson L , Alsammarae D , Vallejo P , Coronado R 2003; Truncation of the carboxyl terminus of the dihydropyridine receptor beta1a subunit promotes Ca²⁺ dependent excitation-contraction coupling in skeletal myotubes. *Biophys J*. 84: 220- 237
- Sheridan DC , Cheng W , Carboneau L , Ahern CA , Coronado R 2004; Involvement of a heptad repeat in the carboxyl terminus of the dihydropyridine receptor beta1a subunit in the mechanism of excitation-contraction coupling in skeletal muscle. *Biophys J*. 87: 929- 942
- Snutch TP , Reiner PB 1992; Ca²⁺ channels: diversity of form and function. *Curr Opin Neurobiol*. 2: 247- 253
- Strube C , Beurg M , Powers PA , Gregg RG , Coronado R 1996; Reduced Ca²⁺ current, charge movement, and absence of Ca²⁺ transients in skeletal muscle deficient in dihydropyridine receptor beta 1 subunit. *Biophys J*. 71: 2531- 2543

Figure 2

Identification of the JP-45 domain interacting with Cav1.1

A. GST-JP-45 fusion proteins encompassing different domains of JP-45 were bound to glutathione-Sepharose beads and incubated with solubilized rabbit skeletal muscle microsomal vesicles as described in the Methods section. The proteins present in the void (V), last wash (LW) and those bound (B) to the beads were separated on a 10% SDS PAG, transferred onto nitrocellulose and the presence of the bound Cav1.1 was revealed by Western blotting using commercial anti- α 1.1 antibodies. B. Co-immunoprecipitation experiment using monoclonal anti-JP-45 Ab to pull down the Cav1.1. Experiments were performed as described in the Methods section: where indicated recombinant GST-JP-45 domain 2 was used to compete out the interaction between endogenous proteins present in the microsomes forming a supramolecular complex.

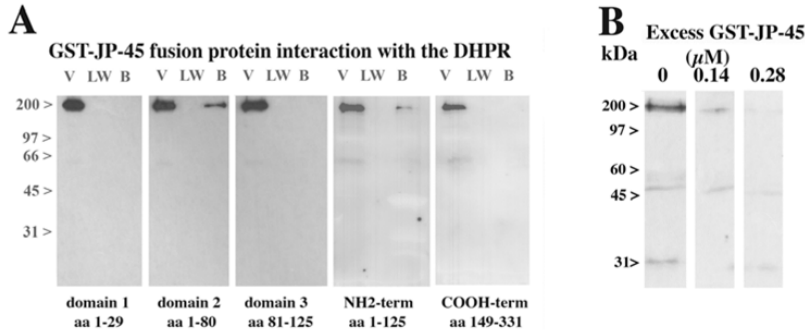


Figure 3

Identification of Cav1.1 domains interacting with JP-45

α 1.1 domains I-II, COOH-distal, COOH-proximal and β 1a interact with the cytosolic domain of JP-45. A. Immunoblot of purified His-tagged fusion proteins encompassing the different α 1.1 domains (10% Tricine SDS PAG) and β 1a (10% SDS PAG). Immunostaining was carried out using commercial anti-poly-His antibodies followed by peroxidase conjugated anti-mouse IgG; bands were visualized by chemiluminescence. B. Pull-down of His-tagged fusion proteins with domain 2 of JP-45 (aa residue 1-80). GST-JP-45 domain 2 fusion protein was bound to glutathione-Sepharose beads and incubated with the His-tagged recombinant α 1.1 proteins. Proteins present in the void (V) or bound to the beads (B) were separated on a 10% tricine SDS PAG or 10% SDS PAG (for the β 1a subunit), blotted onto nitrocellulose and visualized by Western blot using anti-poly-His Ab as described above. C. GST-JP-45 domain 2 fusion protein was bound to glutathione-Sepharose beads and incubated with solubilized light sarcoplasmic reticulum vesicles isolated from rabbit skeletal muscle in the presence of the indicated concentration of competing His-tagged I-II loop or COOH-distal fusion proteins. D. Monoclonal anti-JP-45 antibodies were used to co-immunoprecipitate the complex from solubilized light microsomal vesicles isolated from rabbit skeletal muscle in the presence of the indicated concentration of competing His-tagged I-II loop or COOH-distal fusion proteins. Proteins bound to the beads were separated in a 10% SDS PAG, transferred onto nitrocellulose and probed with anti- α 1.1 antibodies.

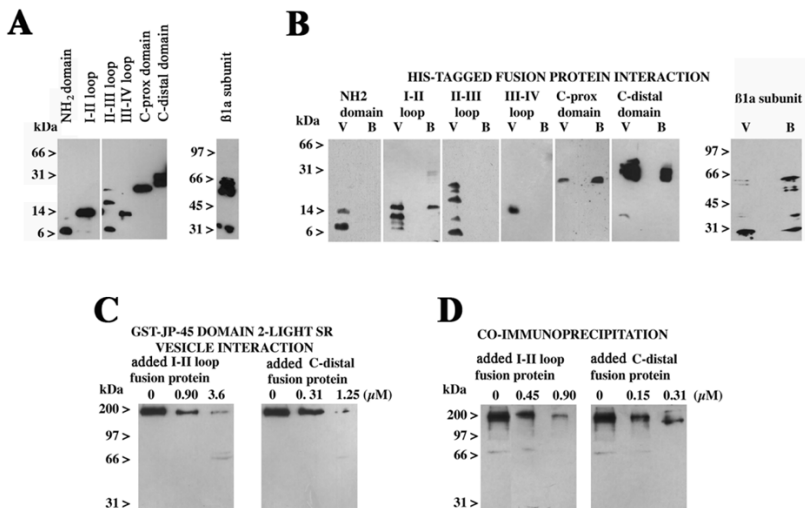


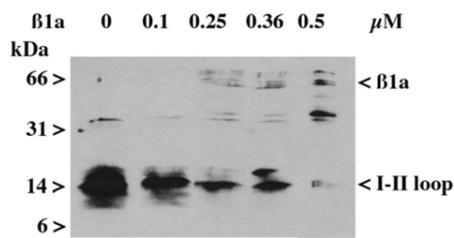
Figure 4

Effect of the β 1a subunit on the interaction between JP-45 and Cav1.1

A. Interaction between GST-JP-45 and His I-II loop in the presence of competing purified β 1a subunit. For the fusion-protein protein interaction, 0.57 μ M of GST-JP-45 domain 2 and 1.4 μ M I-II loop fusion protein were incubated in the presence of the indicated concentration of His-tagged β 1a subunit. His tagged I-II loop fusion proteins bound to the GST-JP-45 domain 2 coated glutathione-Sepharose beads were separated on a 10% tricine SDS PAG and probed with anti-poly-His Ab as described in the legend to figure 3. B. Solubilized rabbit skeletal muscle light sarcoplasmic reticulum vesicles were incubated with GST-JP-45 domain 2-coated glutathione-Sepharose beads in the absence or presence of purified β 1a subunit. Proteins present in the void (V) and bound to the beads (B), were separated on a 10% SDS PAG, blotted onto nitrocellulose and probed with anti- α 1.1 subunit Ab. C. Solubilized rabbit skeletal muscle light sarcoplasmic reticulum vesicles were incubated with anti-JP-45 Ab followed by incubation with Sepharose-protein G beads in the absence or presence of competing purified β 1a subunit. Proteins present in the void (V) and bound (B) to the beads, were separated on a 10% SDS PAG, blotted onto nitrocellulose and probed with anti- α 1.1 subunit Ab.

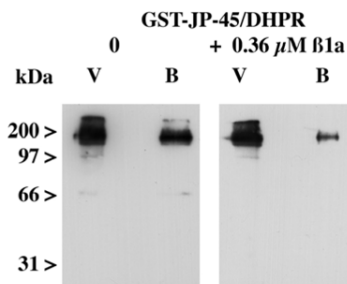
A

FUSION PROTEIN INTERACTION (GST-JP-45/His I-II LOOP \pm β 1a)



B

GST-JP45-LIGHT SR INTERACTION



C

CO-IMMUNOPRECIPITATION

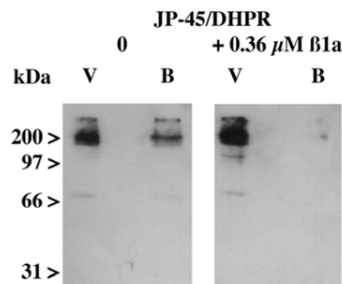
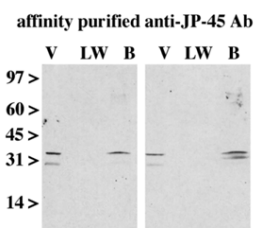


Figure 5

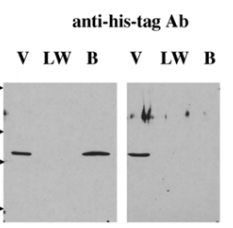
JP-45 interacts with the AID domain on the I-II loop of Cav1.1

A. A GST-I-II loop fusion protein or the GST-AID containing domain encompassed within α 1.1 residues 336-384 were incubated with His-tagged JP-45 domain 2. Pull down was performed as described in figure 3; proteins in the void (V), last wash (LW) or bound (B) to the glutathione resin were separated on a 12.5% SDS PAG, transferred onto nitrocellulose and probed with affinity-purified anti-JP-45 Ab. B. A synthetic biotinylated peptide corresponding to the AID sequence or an unrelated biotinylated peptide were used to coat Neutroavidine beads, which were subsequently incubated with His-JP-45 domain 2. Proteins present in the void, last wash or bound to the beads were separated on a 12.5% SDS PAG, transferred onto nitrocellulose and the immunopositive band was visualized using anti-His-tag commercial Abs. C. A his-tagged fusion protein encompassing domain 2 JP-45 was prepared as described in the Methods section. Though the fusion protein migrated slower in SDS-PAG, its identity was verified by direct sequencing (not shown), by immunoblotting using anti-His Ab. Note that treatment of the fusion protein with DTT+DEPC eliminated its immunoreactivity.

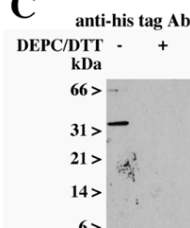
A



B



C



BAIT: GST I-II domain, GST-AID (336-384)
LIGAND: His-JP-45, His-JP-45

biotinylated-AID, biotinylated-unrelated peptide
His-JP-45, His-JP-45

Figure 6

Overexpression of JP-45 in C2C12 cells does not affect the expression level of $\alpha 1.1$ subunit

C2C12 cells were transfected either with the pFP-N3/DsRed2/JP-45 vector or with pFP-N3/DsRed2 alone as control. Panel A- Microsomes were prepared from transfected differentiated C2C12; 5 μ g protein were separated on a 10%SDS PAG, blotted onto nitrocellulose and probed with anti-JP-45 polyclonal Ab, followed by protein G peroxidase. The immunoreactive band was visualized by chemiluminescence. Note that control cells show the endogenous JP-45 immunoreactive band alone, while cells transfected with the pFP-N3/DsRed2/JP-45 vector show an additional band of approximately 70 kDa, representing the DsRed/JP-45 fusion protein. Panel B- immunoprecipitation and Western blot analysis of $\alpha 1.1$ subunit expression in C2C12 cells transfected with pFP-N3/DsRed2 or pFP-N3/DsRed2/JP-45. Results are representative of transfection experiments performed three different times.

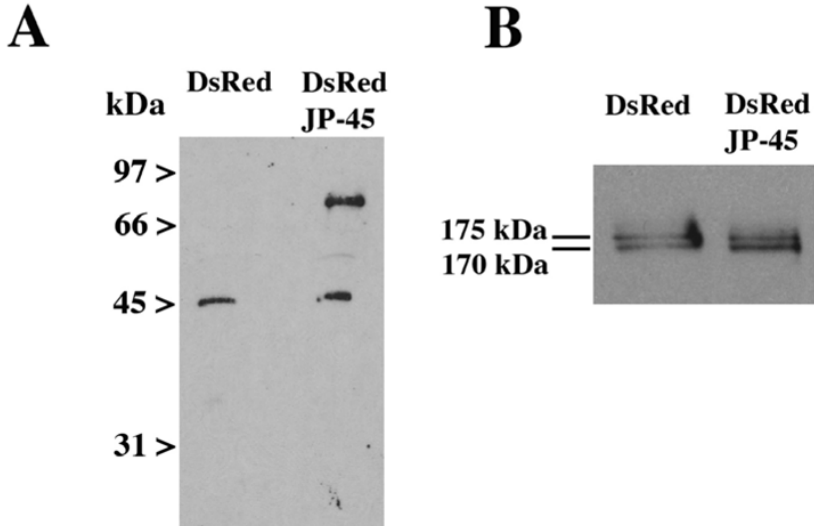


Figure 7

Effect of JP-45 Overexpression on Cav1.1 charge movement

Maximum charge movement – fluorescence relationship for C2C12 cells transfected with either pFP-N3/DsRed2 JP-45 (A) or pFP-N3/DsRed2 alone as control (B). The lines in A and B represent the linear regression including all data points. Charge movement – Vm relationship for pFP-N3/DsRed2 JP-45 (C) or pFP-N3/DsRed2 plasmid (D) transfected cells fitted to a Boltzmann equation 1 (see text). The best fitting parameters are included in Table 1. Charge movement-Vm relationship for the five top and bottom Q_{max} values (E) from JP-45 transfected cells (C).

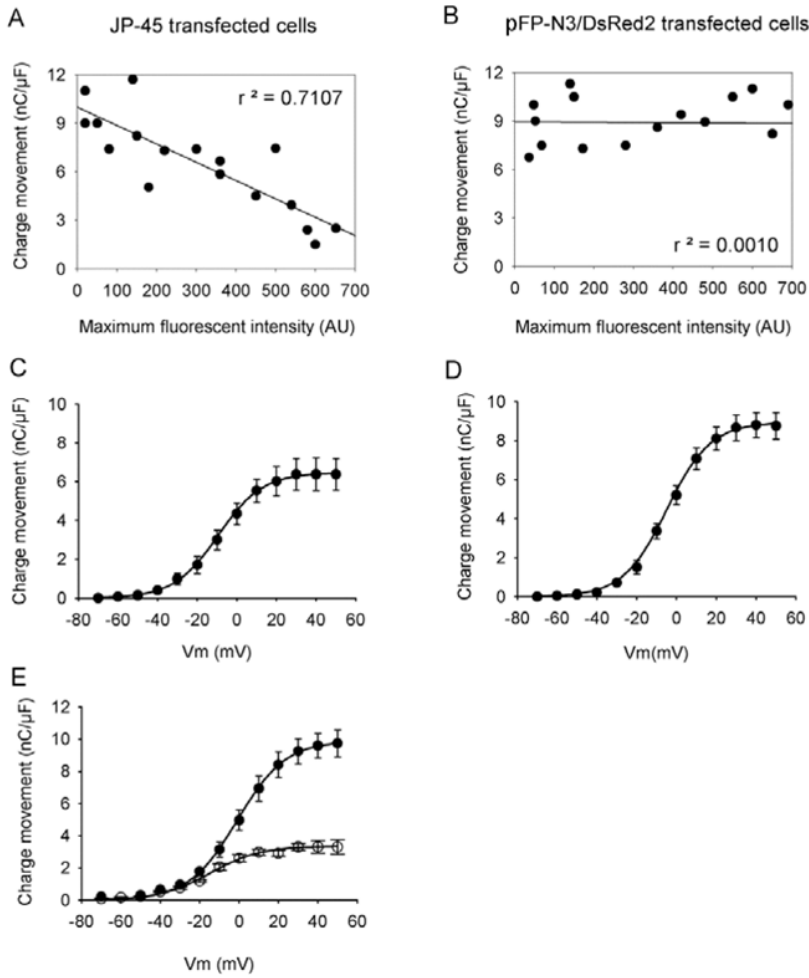


Figure 8

JP-45 gene silencing in differentiated C2C12 myotubes

A. Total RNA was extracted from transfected and differentiated C2C12 cells, converted into cDNA and the cDNA encoding JP-45 and β -actin was amplified by PCR. Amplified DNA obtained from 50 or 100 ng RNA was separated on a 7.5% acrylamide gel (JP-45, Top Panel) or a 1% agarose gel (β -actin, Bottom Panel). B. Microsomal proteins from transfected and differentiated C2C12 cells were prepared, separated on a 10% SDS PAG, blotted onto nitrocellulose and probed with anti-JP-45 Abs (central panel) or commercial anti- β -actin Abs, followed by peroxidase-labelled secondary Abs. Immunoreactive bands were visualized by chemiluminescence. Panel on the right shows blotted proteins stained with Ponceau Red. Results are representative of experiments carried out on three different transfection experiments.

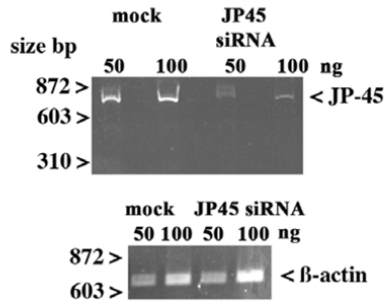
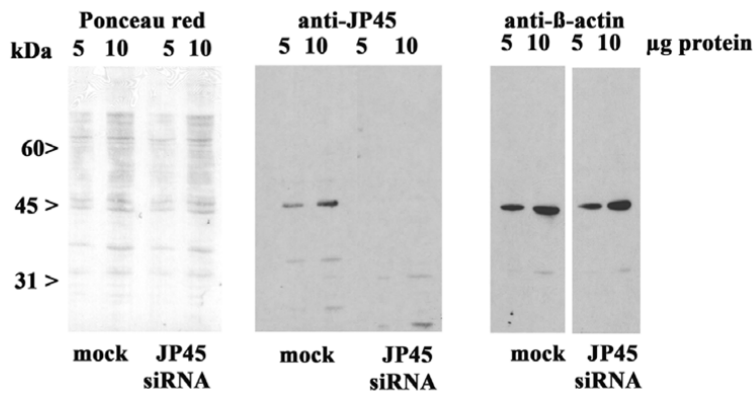
A**B**

Figure 9**JP-45 gene silencing modifies Cav1.1 charge movement**

Charge movement – membrane voltage (Vm) relationship recorded in C2C12 cells transfected with JP-45 siRNA (triangles) (n = 18). Control cells were transfected with pSHAG vector (circles) (n = 17). A illustrate data points, expressed as means \pm S.E.M., were fitted to a Boltzmann equation (equation 1). B and C illustrate charge movement records in the -30 to +30mV range. Numbers on the left indicate the membrane potential. Dotted lines represent the baseline. D and E show immunoprecipitation and western blot analysis of Cav1.1 α 1 subunit expression in C2C12 cells transfected with siRNA JP-45 and control pSHAG vector. D and E represent two from a total of 4 assays. The Cav1.1 α 1 subunit expression in D and E decreased by 69 and 28%, respectively. The location of the molecular weight standards and their M_r values are depicted on the right.

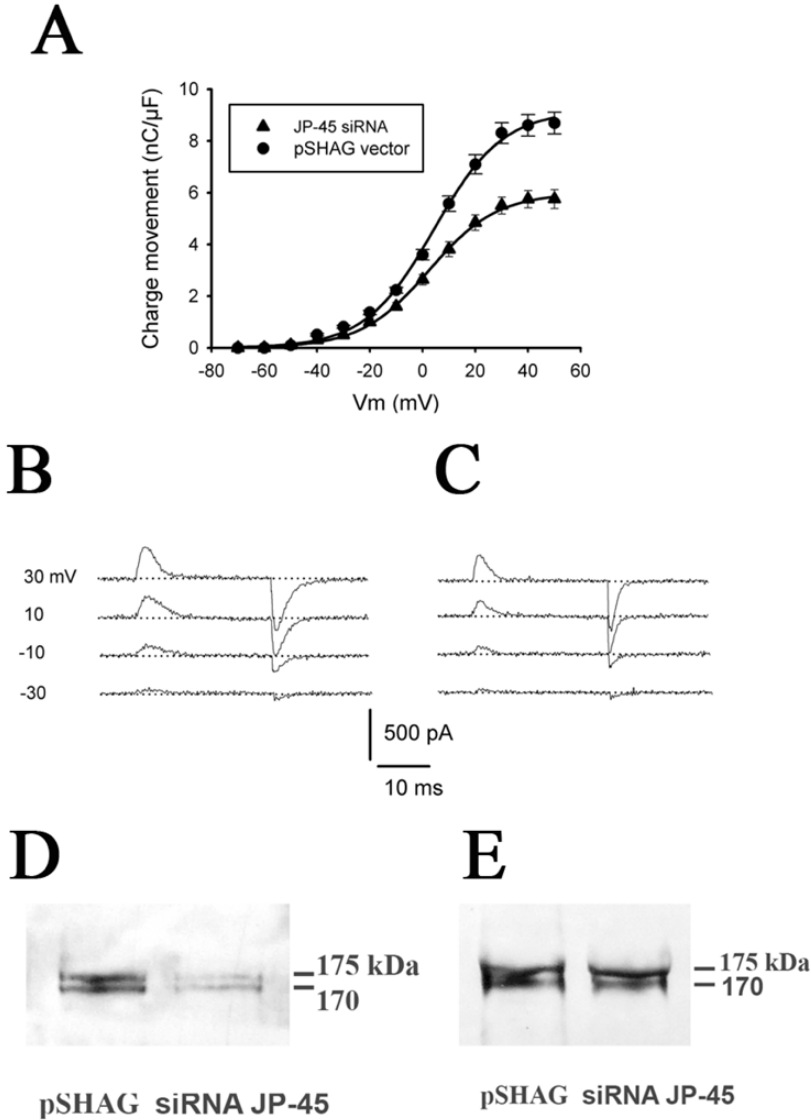


Figure 10

Model depicting potential functional role of JP-45

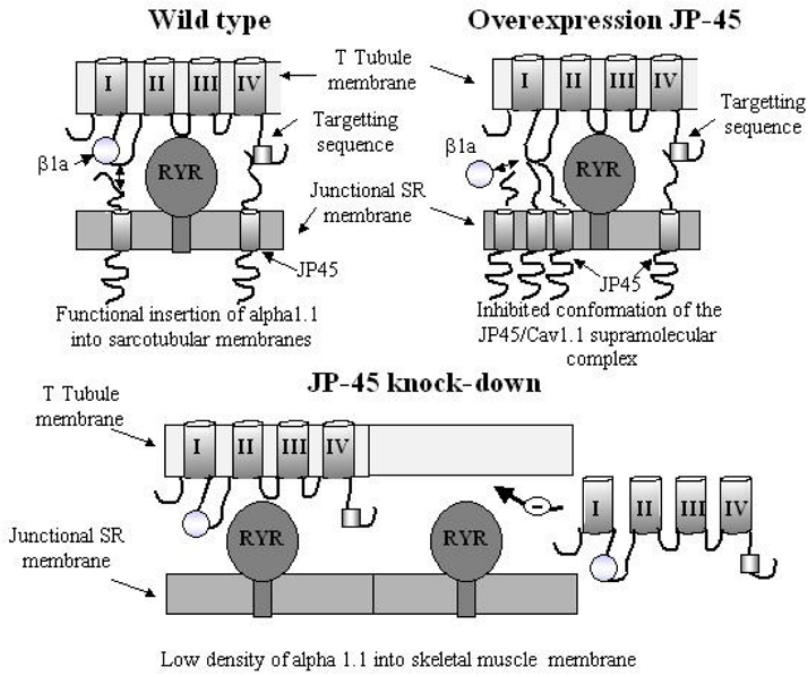


TABLE 1

Best-fitting parameters describing the voltage-dependence of charge movement in JP-45 overexpressing C2C12 myotubes

	Best-fitting parameters		
	Q_{\max} (nC μF^{-1})	$V_{Q1/2}$ (mV)	K
JP-45 transfected cells N = 17	6.4 ± 0.3	-9.1 ± 1.2	11.4 ± 1.5
Only vector transfected cells N = 15	8.9 ± 0.3 (*)	-5.1 ± 0.7 (*)	10.7 ± 1.1 (ns)
JP-45 Max Q values (n = 5)	10.1 ± 1.0	-3.2 ± 0.03	12.5 ± 0.6
JP-45 Min Q values (n = 5)	3.2 ± 0.04 (**)	-14.5 ± 0.13 (**)	12.5 ± 0.5 (ns)

Statistically significant difference between cells transfected with either JP-45 or only vector (*) and between JP-45 maximum (Max) and minimum (Min) charge movement (Q) values (**) ($P < 0.05$). N, number of cells. ns, not significant. Values are mean ± SEM.

TABLE 2

Best-fitting parameters describing the voltage-dependence of charge movement in JP-45 siRNA and pSHAG transfected C2C12 myotubes

	Best-fitting parameters		
	Q_{\max} (nC μF^{-1})	$V_{Q1/2}$ (mV)	K
JP-45 siRNA N = 18	5.8 ± 0.37	-2.1 ± 0.03	12.9 ± 0.6
pSHAG vector N = 17	8.7 ± 0.41 *	-3.2 ± 0.04	13.0 ± 0.7

Values are means ± SEM. N, number of cells. Values are mean ± SEM.

* $P < 0.05$